Available online at www.sciencedirect.com

ScienceDirect

IFAC PapersOnline CONFERENCE PAPER ARCHIVE

IFAC PapersOnLine 54-3 (2021) 231–236

Control of Particle Formation Processes

Eric Otto * **Jessica Behrens** *,** **Robert Dürr** ** **Stefan Palis** ***
Achim Kienle *,**

* *Otto-von-Guericke-University Magdeburg, D-39106 Magdeburg*
** *Max-Planck-Institute for Dynamics of Complex Technical Systems, D-39106 Magdeburg*
*** *Moscow Power Engineering Institute, Moscow, Russia*

Abstract: Discrepancy-based control (DBC) represents an elegant direct control design concept for infinite-dimensional systems, which is frequently used to control particle formation processes, an important class of operations in chemical engineering. So far, DBC has been applied to continuous layering growth and agglomeration, which have been accounted for by partial differential equations. In this contribution we develop control laws for infinite systems of ordinary differential equations, inspired by DBC. The results are visualized by the application to a continuous agglomeration process involving additional particle breakage. We show how a two-dimensional controller is able to control the industrially relevant Sauter mean diameter of the product particles, resulting in improved performance of the closed-loop system compared to a single control loop.

Keywords: Population Balance Modeling, Particle Formation, Agglomeration, Breakage, Discrepancy-based control

1. INTRODUCTION

Particle formation processes such as granulation, polymerization, and crystallization are widespread unit operations in industrial processes, producing versatile goods, such as pharmaceuticals, fertilizers, synthetics, food powders and many more. Those formation processes have the same mechanistic subprocesses in common, such as nucleation, growth, agglomeration (or aggregation, coagulation) and breakage (or fragmentation) and can therefore be treated similarly from an engineering perspective. The resulting particle collectives are characterized by distributions of relevant particle properties such as size and shape as well as composition for polymers, porosity for granules and crystallinity for crystals. The production of particles with desired product properties is a common goal of the processes, since these properties define the quality of the manufactured product, which also explains the high research interest in this direction (Litster and Ennis, 2013; Crowley et al., 2000; Ramkrishna and Mahoney, 2002).

A powerful tool to ensure the desired product quality on the one hand and to optimize the production process on the other hand is model-based process control. In order to implement advanced control strategies, suitable dynamical process models are required. An established framework is population balance modelling (Ramkrishna, 2000), where the process dynamics are usually expressed by nonlinear partial differential equations (PDEs) or less often by high-dimensional systems of ordinary differential equations (ODEs). The formulation as PDEs makes control tasks challenging, since there are no standard feedback control methods available for such nonlinear infinite-dimensional problems. Nevertheless, a variety of approaches is presented in the literature. Since this contribution focuses on the particle size as one of the most important particle properties, the following overview will be restricted to control of particle size distributions. However, most of the methods can be applied to any distributed particle property.

The aim of this contribution is to design a control law for an infinite system of ODEs, inspired by the discrepancy-based control approach and to apply it to a particle formation process. An extended and discrete version of the population balance example from Otto et al. (2021) is used as an example process. Finally, it is shown that the control methodology can be used to control an industrially relevant particle property.

The remainder of this paper is structured as follows: In the second section, the population balance equation (PBE) for the agglomeration and breakage process is presented and the control design procedure is introduced briefly. In the third section, the control laws are derived and verified by simulation. The last section summarizes the results and gives an overview of further possible research directions.

2. METHODS

In this section a simple process model, including particle agglomeration and breakage, is presented. Furthermore, the control design procedure based on the discrepancy-based control approach is reviewed briefly.

2.1 Process Model

As an example for a particle process a continuous agglomeration process is chosen. It is an industrial process commonly used to increase the size of particles. During an agglomeration process, which is often performed in a

10.1016/j.ifacol.2021.08.247

drum (Walker, 2007) or a fluidized bed (Peglow et al., 2007), particles can form agglomerates after collision. The aggregation can have multiple causes, e.g. binder induced formation of liquid or solid bridges between particles or different kinds of interparticle forces. Usually, binary aggregation is considered, i.e. particles of volume u and $v-u$ form a particle of volume v. Another typical sub-process occurring is binary particle breakage. Due to external forces on the particle, e.g. collision with another particle, an agglomerate of volume v breaks into two smaller particles.

These processes can be described mathematically using the population balance framework (Ramkrishna, 2000). Here, particle properties are represented by internal coordinates that can be either continuous or discrete. In this contribution, the particle volume v is considered, as characteristic particle property. It is assumed that all agglomerates are composed of a number of equally sized primary particles with volume v_0

$$v_i = i\ v_0\,, \quad i \in \mathbb{N} \tag{1}$$

The particle ensemble can be described by the corresponding number density distribution $n(t, v)$, which characterizes the number of particles with volume v at time t. The number of particles with size v_i is consequently given by $n(t, v_i)$ and will be abbreviated with $n_i(t)$ in the remainder of this manuscript. The evolution of n (and n_i) is characterized by aggregation (A) and breakage (B) as well as a primary particle feed (F) and a product particle withdrawal (O) in the continuous operation mode. A schematic presentation of the process is given in Fig. 1. The resulting PBE is given by an infinite-dimensional system of ODEs

$$\frac{\mathrm{d}n_i}{\mathrm{d}t} = F_i(t) + A_i(t) + B_i(t) - O_i(t)\,, \quad i \in \mathbb{N} \tag{2}$$

The four terms on the right-hand-side, representing the sub-processes described above, are explained briefly in the following.

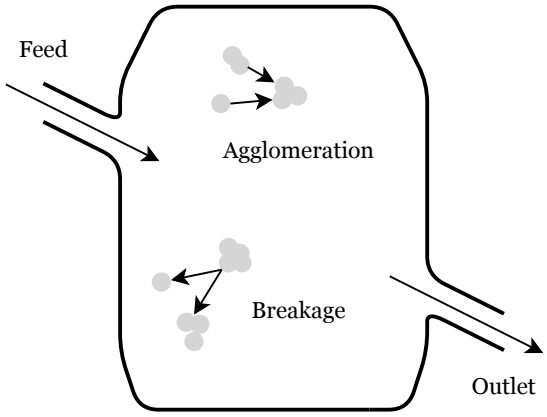

Fig. 1. Schematic representation of the process.

The particle feed F_i is given by

$$F_i(t) = f(t)\tilde{n}_{i,\mathrm{f}} \tag{3}$$

where f is the time-dependent (and size-independent) feed rate and $\tilde{n}_{i,\mathrm{f}}$ is the i-th element of the normalized primary particle distribution.

The agglomeration term is given by

$$A_i(t) = \frac{1}{2}\sum_{j=1}^{i-1} a_{j,i-j} n_j(t) n_{i-j}(t) - n_i(t)\sum_{j=1}^{\infty} a_{i,j} n_j(t) \tag{4}$$

where $a_{i,j}$ is the agglomeration kernel which represents the rate of agglomeration for particle pairs with volume v_i and v_j. For more information regarding the agglomeration term the readers are referred to Narni et al. (2012).

The rate of breakage for a particle with volume v_i is given by

$$B_i = \sum_{j=i+1}^{\infty} b_{i,j} s_j n_j - s_i n_i. \tag{5}$$

Here, s_j denotes the selection rate, which describes the rate at which a particle of volume v_j breaks into smaller fragments. The breakage kernel $b_{i,j}$ denotes the probability that a particle of volume v_j breaks into a particle of volume v_i. Since breakage is assumed to be binary and volume-conserving, the second particle has volume v_{j-i}. Since it is desirable to only withdraw particles from the process that exceed a specified volume, the particle outlet is assumed to be classifying with a separation function $T_i := T(v_i)$. Here, we choose T to be a cumulative Gaussian function with mean value μ_s and variance σ_s. The outlet term is then given by

$$O_i(t) = K(t) T_i n_i \tag{6}$$

with the withdrawal rate $K(t)$. It is assumed that K is a plant parameter that can be manipulated freely.

It is worth mentioning that the presented process model represents the discrete version of the continuous one proposed in (Otto et al., 2021).

2.2 Control Design Method

Discrepancy-based control is a stability-based control approach for PDEs (Movtschan, 1960; Sirazetdinov, 1967). It relies on a stability notion where the "distance" between the state of a process and its equilibrium is not measured using metrics but a generalized distance measure, the so-called discrepancy. In the finite dimensional case, the discrepancy can be interpreted simply as system output and can be stabilized (asymptotically) using control Lyapunov functions. The distribution is then (asymptotically) stable if the zero-dynamics are (asymptotically) stable.

In Palis and Kienle (2012); Geyyer et al. (2017) and Otto et al. (2021), moments of particle size distributions have been shown to be useful control variables. The k-th moment of a particle size distribution is defined as

$$\mu_k(t) = \int_0^\infty x^k n(t, x)\,\mathrm{d}x \tag{7}$$

for continuous variables x. If x is the particle volume v, the zeroth moment is proportional to the total number of particles N_tot, the first moment is proportional to the total particle volume V_tot and the moment with $k = 2/3$ is proportional to the total particle surface A_tot. In Otto et al. (2021), for example, the discrepancy

$$\rho(n, t) = \left(\mu_{0,\mathrm{d}} - \mu_0(t)\right)^2 \tag{8}$$

is utilized, where $\mu_{0,\mathrm{d}}$ is the desired steady state value of the zeroth moment. In order to apply the DBC-concept to

the discrete PBE formulation, we simply use the discrete moments

$$\mu_k(t) = \sum_{i=1}^{\infty} x_i^k n_i(t) \tag{9}$$

as system outputs and control variables. Then the control design effort is reduced to finding suitable Lyapunov functions and, if possible, showing stability of the zero-dynamics.

3. RESULTS

In the following, a two-dimensional control law for the PBE (Equ. 2) is derived. Afterwards the control law is tested in a simulation scenario and discussed in terms of dynamics and convergence.

3.1 Derivation of the Control Law

Particle size distributions are often represented by mean values. In particular the Sauter mean diameter d_{32} is frequently used in industrial applications. It represents the mean diameter of a collection of particles of different sizes that is equal to the diameter of equisized spherical objects forming a collection with same total volume and same total surface. For the discrete particle size distribution, it can be defined as

$$d_{32}(t) = 6\frac{V_{tot}}{A_{tot}} = 6^{5/3}\pi^{2/3}\frac{\mu_1(t)}{\mu_{2/3}(t)} = 6^{5/3}\pi^{2/3}\frac{\sum_{i=1}^{\infty} v_i n_i(t)}{\sum_{i=1}^{\infty} v_i^{\frac{2}{3}} n_i(t)} \tag{10}$$

and therefore represents the ratio of the first moment μ_1 to the 2/3th moment $\mu_{2/3}$. Controlling the Sauter mean diameter as a measure of product quality therefore requires controlling both moments and a two-dimensional control law. It is derived using two commonly accessible parameters as manipulated variables: the withdrawal rate $K(t)$ is used to control μ_1 and the feed rate $f(t)$ to control $\mu_{2/3}$. It is intuitively clear that the total particle surface is highly sensitive to the rate at which particles with low diameter and high relative surface are fed to the process. Likewise, the total particle volume is more sensitive to the rate at which large particles are withdrawn, since a fixed number of large particles has a higher volume than a fixed number of smaller particles. The control errors are therefore defined by

$$e_{2/3}(t) = \sum_{i=1}^{\infty} v_i^{\frac{2}{3}}(n_{d,i}(t) - n_i(t)) \tag{11}$$

$$e_1(t) = \sum_{i=1}^{\infty} v_i(n_{d,i}(t) - n_i(t)) \tag{12}$$

where n_d denotes the desired number distribution, which is assumed to be constant with respect to time. The following control design procedure consists of two steps: At first, a controller for $\mu_{2/3}$ is derived. Afterwards, the resulting closed-loop system is used to calculate the controller for μ_1. The final control structure is shown schematically in Fig. 2.

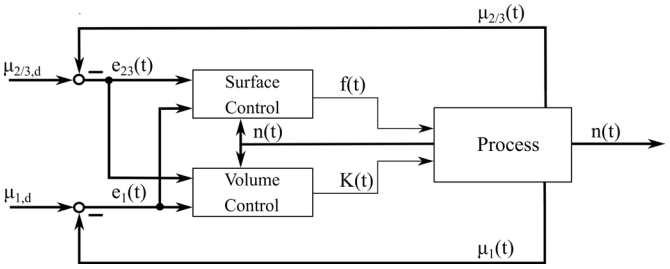

Fig. 2. Two-dimensional control scheme.

Now the following Lyapunov-functional is used to derive the first stabilizing controller:

$$V_{2/3} = \frac{1}{2}e_{2/3}^2. \tag{13}$$

Calculating its time derivative yields

$$\dot{V}_{2/3} = -e_{2/3}\left(f(t)\,w + \sum_{i=1}^{\infty} v_i^{\frac{2}{3}}(A_i + B_i - KT_i n_i)\right)$$

where w is defined as

$$w = \sum_{i=1}^{\infty} v_i^{\frac{2}{3}} \tilde{n}_{i,\mathrm{f}}\,. \tag{14}$$

By choosing

$$f(t) = \frac{1}{w}\left(c_{2/3}e_{2/3} - \sum_{i=1}^{\infty} v_i^{\frac{2}{3}}(A_i + B_i - KT_i n_i)\right) \tag{15}$$

the time derivative of the Lyapunov-functional results in

$$\dot{V}_{2/3} = -2\,c_{2/3}V_{2/3}, \tag{16}$$

which shows that the controller exponentially stabilizes $\mu_{2/3}$. The positive constant $c_{2/3}$ is a tuning parameter for the convergence speed of control loop. Now the second control law for μ_1 is derived using the following Lyapunov-functional

$$V = \frac{1}{2}(e_{2/3}^2 + e_1^2). \tag{17}$$

Calculating the time derivative of V and introducing equations (2) and (15) yields

$$\begin{aligned}\dot{V} = &- c_{2/3}e_{2/3}^2 - e_1\Bigg[\sum_{i=1}^{\infty} v_i\Bigg(\frac{\tilde{n}_{i,\mathrm{f}}}{w}\Big(c_{2/3}e_{2/3} \\ &- \sum_{j=1}^{\infty} v_j^{\frac{2}{3}}(A_j + B_j)\Big) + A_i + B_i\Bigg) + \\ &K\sum_{i=1}^{\infty} v_i\Bigg(-T_i n_i + \frac{\tilde{n}_{i,\mathrm{f}}}{w}\sum_{j=1}^{\infty} v_j^{\frac{2}{3}}T_j n_j\Bigg)\Bigg].\end{aligned} \tag{18}$$

The choice

$$\begin{aligned}K = &\left[\sum_{i=1}^{\infty} v_i\left(-T_i n_i + \frac{\tilde{n}_{i,\mathrm{f}}}{w}\sum_{j=1}^{\infty} v_j^{\frac{2}{3}}T_j n_j\right)\right]^{-1} \\ &\Bigg[c_1 e_1 - \sum_{i=1}^{\infty} v_i\Bigg(\frac{\tilde{n}_{i,\mathrm{f}}}{w}\Big(c_{2/3}e_{2/3} - \sum_{j=1}^{\infty} v_j^{\frac{2}{3}}(A_j + B_j)\Big) \\ &+ A_i + B_i\Bigg)\Bigg]\end{aligned} \tag{19}$$

results in

$$\dot{V} = -c_{2/3}e_{2/3}^2 - c_1 e_1^2 \tag{20}$$

and therefore asymptotic stability of the closed-loop system. The positive parameter c_1 is used again as tuning constant.

The presented control law derivation results in a decoupled control system, which is shown by the final control error dynamics

$$\dot{e}_{2/3} = -c_{2/3} e_{2/3} \tag{21}$$

$$\dot{e}_1 = -c_1 e_1, \tag{22}$$

which are obtained by differentiating Equ. (12) and (11), and introducing equations (2), (15) and (19). In addition, the derivation is independent of the agglomeration and breakage kernel and can therefore be applied to a wide spectrum of particle population balance models.

3.2 Simulation

The control law is now applied to the process described in section 2.1. Before the simulation results are presented, the rate constants as well as the feed distribution and the separation function for the example process are given.

The normalized primary particle distribution is chosen as a decaying exponential function:

$$\tilde{n}_{i,\mathrm{f}} = \frac{\exp(-v_i)}{\sum_{i=1}^{\infty} \exp(-v_i)}, \quad i \in \mathbb{N}. \tag{23}$$

For the agglomeration kernel $a_{i,j}$, the discrete formulation of the well-known Kapur-kernel (Kapur and Fuerstenau, 1969)

$$a_{i,j} := a(v_i, v_j) = \alpha_0 \frac{(v_i + v_j)^{\alpha_1}}{(v_i v_j)^{\alpha_2}}, \quad (i,j) \in \mathbb{N}^2 \tag{24}$$

with the agglomeration efficiency α_0 and two empirical parameters α_1 and α_2 is chosen.

Regarding particle breakage the selection function and breakage kernel are chosen as

$$s_j = \beta_0 v_j^{2/3}, \quad j \in \mathbb{N} \tag{25}$$

and

$$b_{i,j} = \delta_{i,1} + \delta_{i,j-1}, \quad (i,j) \in \mathbb{N}^2 \tag{26}$$

respectively. Here, $\delta_{i,j}$ denotes the Kronecker delta. Equ. (26) reflects the fact that a particle of volume v_j breaks into two fragments of volumes v_1 and v_{j-1}.

The system of ODEs given by Equ. (2) is solved using the ODE-solver *ode15s* within the MATLAB environment. For the simulation, $N = 300$ particle volumes are assumed. In the following a shift of the operating point is simulated both in open- and closed-loop operation. In the first case, the nominal withdrawal rate K_{nom} is increased to $10K_{\mathrm{nom}}$ at $t = 1$ while f_{nom} stays constant. In the latter case, the inputs are determined by the controller and limited by f_{max} and K_{max} from above and by zero from below in order to establish typical practical constraints for such a control scenario. The initial particle size distribution for both scenarios is given by the steady state distribution for f_{nom} and K_{nom}. The tuning parameters c_1 and $c_{2/3}$ were determined iteratively. The complete set of simulation parameters is given in Tab. 1. Note that all parameters and the process time are unitless, since the simulation example does not represent a specific process plant.

Tab. 1. Simulation parameters

Parameter	Value	Parameter	Value
μ_{s}	255	σ_{s}	30
f_{nom}	$1 \cdot 10^7$	K_{nom}	2
$f_{\max}$	$2 \cdot f_{\mathrm{nom}}$	$K_{\max}$	$15 \cdot K_{\mathrm{nom}}$
β_0	$1 \cdot 10^{5}$	α_0	$9 \cdot 10^{8}$
α_1	1	α_2	0.1
$c_{2/3}$	$1 \cdot 10^1$	c_1	$1 \cdot 10^5$
v_0	1		

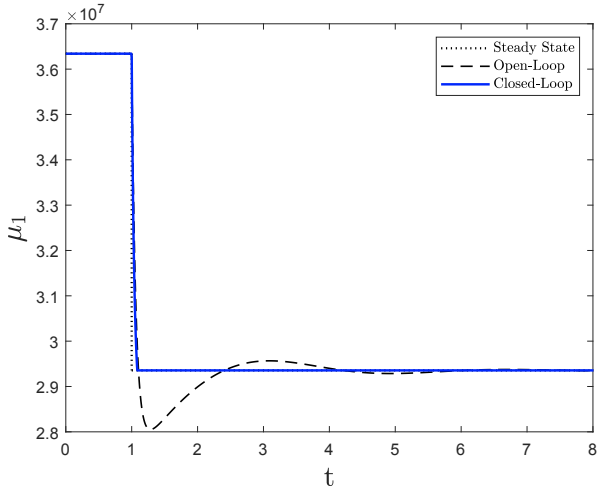

Fig. 3. Time evolution of the first moment of the open-loop (black dashed line) and closed-loop system (blue solid line) for an operating point change

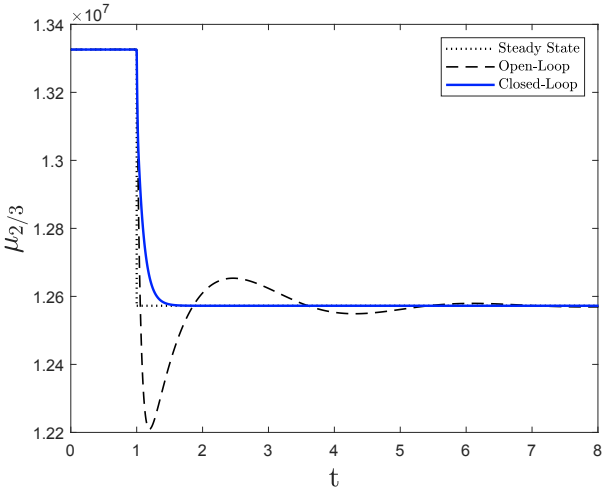

Fig. 4. Time evolution of the 2/3th moment of the open-loop (black dashed line) and closed-loop system (blue solid line) for an operating point change.

Fig. 3 and Fig. 4 present the evolution of the first and the 2/3th moment for both scenarios. The controller eliminates oscillations and reaches the desired set point faster. The normalized control inputs are shown in Fig. 5. Note that, while the moments are already in steady state at around $t = 1.5$, the manipulated variables, especially K, are not. This is due to the fact that while stabilizing the outputs, the control law does not guarantee stability of the distribution with respect to a norm. It follows, among other things, that K and n still change while the moments are already in the steady state. From a mathematical

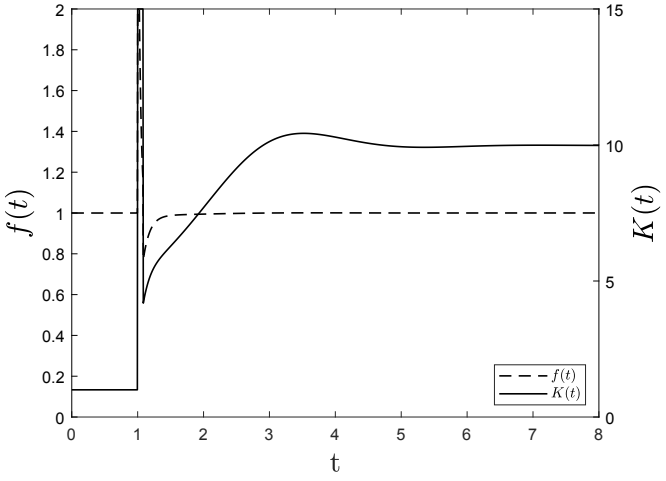

Fig. 5. Normalized control inputs: $f(t)$ (dashed) and $K(t)$ (solid).

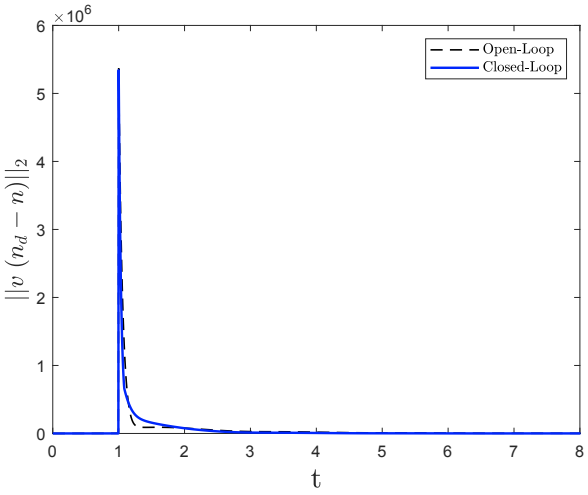

Fig. 6. Convergence in the weighted $\mathrm{L}_{2,w}$ norm of the open-loop (black dashed line) and closed-loop system (blue solid line) for an operating point change.

perspective this is rooted in the fact that a finite number of moments does not determine a distribution uniquely.

In order to further investigate this, the volume weighted L_2 norm of the error distribution

$$\mathrm{L}_{2,w}^2 = \sum_{i=1}^{\infty} \left(v_i(n_{d,i} - n_i)\right)^2 \tag{27}$$

is computed and presented in Fig. 6. It can be seen that the closed-loop process converges also with respect to this norm, i.e. the zero-dynamics of the closed-loop system are asymptotically stable for this example, however the speed of convergence is smaller for the distribution than for the moments. Finally, the d_{32} is analyzed as it was our motivation to introduce a two dimensional control law. In Fig. 7, the closed-loop is compared to the open-loop scenario. Clearly, the Sauter mean diameter converges faster with control. In order to show that the introduction of a second control loop improves the performance, the evolution of d_{32} where only the $\mu_{2/3}$-control-loop is closed is presented. The two-dimensional controller achieves bet-

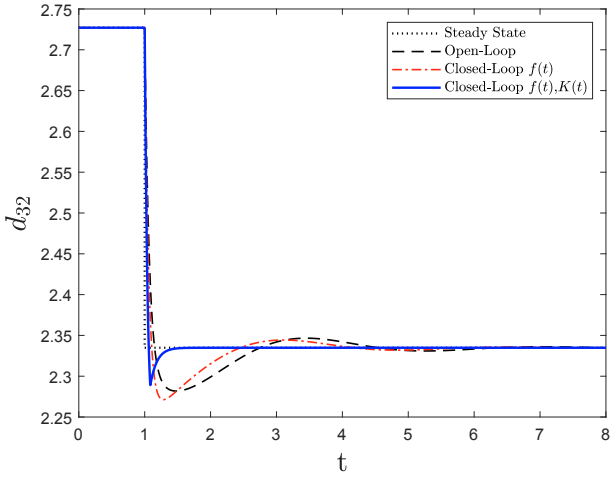

Fig. 7. Time evolution of the Sauter mean diameter for an operating point change. The open-loop system (black dashed line) is compared to a single controller (red dot dashed line) and the derived (blue solid line) control system.

ter results then the one-dimensional controller with respect to convergence speed.

4. CONCLUSION

This contribution was concerned with control of particle formation processes that are modelled mathematically by infinite-dimensional systems of ODEs. The control strategy was inspired by discrepancy-based control and is based on the choice of moments as control variables. It has been shown that an industrially relevant particle property can be controlled by introducing a two-dimensional control law. Furthermore, numerical simulation results show that the particle size distribution is stabilized and that the time of convergence is improved significantly compared to the open-loop case.

Future research should be concerned with further analysis of the zero-dynamics of the system and the practical implementation of the proposed control algorithm at an actual plant. This includes investigation of controller performance under model-plant mismatch. Furthermore, the control approach can be generalized to process models which account for more than one particle properties, e.g. particle porosity.

ACKNOWLEDGEMENTS

This work is funded by the European Regional Development Fund (ERDF) project “Center of Dynamic Systems” The financial support is hereby gratefully acknowledged.

REFERENCES

Crowley, T.J., Meadows, E.S., Kostoulas, E., and Doyle III, F.J. (2000). Control of particle size distribution described by a population balance model of semibatch emulsion polymerization. *Journal of Process Control*, 10(5), 419 – 432.

Geyyer, R., Dürr, R., Temmel, E., Li, T., Lorenz, H., Palis, S., Seidel-Morgenstern, A., and Kienle, A. (2017).

Control of continuous mixed-solution mixed-product removal crystallization processes. *Chemical Engineering & Technology*, 40(7), 1362–1369.

Kapur, P.C. and Fuerstenau, D.W. (1969). Coalescence model for granulation. *Industrial & Engineering Chemistry Process Design and Development*, 8(1), 56–62.

Litster, J. and Ennis, B. (2013). *The Science and Engineering of Granulation Processes (Particle Technology Series Book 15)*. Springer Netherlands.

Movtschan, A. (1960). Stability of processes with respect to two metrics [in Russian]. *Journal of Applied Mathematics and Mechanics*, 24, 988–1001.

Narni, N.R., Warnecke, G., Kumar, J., Peglow, M., and Heinrich, S. (2012). Some modelling aspects of aggregation kernels and the aggregation population balance equations. In J. Mathew, P. Patra, D.K. Pradhan, and A.J. Kuttyamma (eds.), *Eco-friendly Computing and Communication Systems*, 319–326. Springer, Berlin, Heidelberg.

Otto, E., Palis, S., and Kienle, A. (2021). *Stabilization of Distributed Parameter Systems: Design Methods and Applications*, chapter Nonlinear Control of Continuous Fluidized Bed Spray Agglomeration Processes, 73–87. Springer International Publishing.

Palis, S. and Kienle, A. (2012). Discrepancy based control of continuous fluidized bed spray granulation with internal product classification. *IFAC Proceedings Volumes*, 45(15), 756–761.

Peglow, M., Kumar, J., Hampel, R., Tsotsas, E., and Heinrich, S. (2007). Towards a complete population balance model for fluidized-bed spray agglomeration. *Drying Technology*, 25(7-8), 1321–1329.

Ramkrishna, D. (2000). *Population Balances: Theory and Applications to Particulate Systems in Engineering*. Academic Press.

Ramkrishna, D. and Mahoney, A.W. (2002). Population balance modeling. Promise for the future. *Chemical Engineering Science*, 57(4), 595–606.

Sirazetdinov, T. (1967). On the theory of stability of processes with distributed parameters [in Russian]. *Journal of Applied Mathematics and Mechanics*, 31, 36–47.

Walker, G.M. (2007). Chapter 4 drum granulation processes. In A. Salman, M. Hounslow, and J. Seville (eds.), *Granulation*, volume 11 of *Handbook of Powder Technology*, 219–254. Elsevier Science B.V.